sciendo

Polish Journal of Chemical Technology, 23, 2, 1—11, 10.2478/pjct-2021-0010

A mathematical model of two-stage Solid Oxide Fuel Cell, SOFC, stacks for dynamic simulation of Combined Heat and Power system fed by natural gas

Mateusz Palus, Paulina Pianko-Oprych*

West Pomeranian University of Technology, Szczecin, Department of Chemical Engineering and Processes, Faculty of Technology and Chemical Engineering, al. Piastów 42, 71-065 Szczecin, Poland
**Corresponding author: e-mail: paulina.pianko@zut.edu.pl*

Zero-dimensional two-stage SOFC stacks dynamic model was developed to investigate the effect of operating parameters on stacks performance. The model resolves spatially thermal and thermo-electrochemical behaviour for electrochemical reactions, Catalytic Partial Oxidation and Steam Reforming processes. Design variables and thermo-electrochemical properties were obtained from in-house-fabricated SOFCs carried out by project partners. The completed SOFCs based Combined Heat and Power, CHP, system model was validated by data[18] and numerical results obtained at steady-state mode showing its high-fidelity. A parametric study with respect to key operating parameters including changes in fuel utilization, lambda number and current density values was conducted. The global CHP system dynamic response, in term of the current/voltage delivered by two-stage SOFC stacks, under a fixed fuel utilization, has been determined resulting in greater variations in the voltage of a single cell in the first stack in comparison to the corresponding values in the second stack.

Keywords: dynamic model, natural gas, Solid Oxide Fuel Cell stacks, Combined Heat and Power, CHP, system, Balance of Plant, BoP, modelling, Catalytic Partial Oxidation, CPO_x, reformer, steam reformer.

INTRODUCTION

Depletion of fossil fuels and continuous increase in level of environmental pollutions led to the need for the development of alternative forms of energy generation and energy storage. Several studies have been carried out in the direction of data[18] and numerical work on energy management using hybrid systems including the use of Solid Oxide Fuel Cells, SOFCs[1–2]. It is well known that Combined Heat and Power, CHP, systems based upon the use of SOFCs have the capability to achieve greater than 70% overall system efficiency by generating power near the point of use and recovering the waste heat. High fuel conversion efficiency to electricity and extremely low emissions make SOFC based CHP systems particularly attractive. Moreover, two other less obvious SOFC attributes made hybrid systems valuable such as SOFC inherent transient performance capability and increased efficiency at part load[3]. To obtain these benefits from the use of the fuel cells, several factors must be met. According to Ferrari[4], the SOFC performance in the system is affected by the conditions at which it operates such as fuel cell temperature (maximum gradient significantly lower than 3 K/min), the pressure gap between cathode and anode sides (at least a 30% decrease during transient operations) and controlling Steam-to-Carbon ratio, S/C, for safety issues. These constraints have to be considered not only for steady-state conditions but also during time-dependent operations[5]. In addition, during time-dependent operations other risk situations must be addressed such as load variations, ambient temperature changes and start-up/shut down phases[6]. Padulles et al.[7] were among the first who carried out dynamic simulations to define what were the safe operating areas of the plant under three different limits including underused fuel, overused fuel and undervoltage. In numerical study Padulles et al.[7] used MATLAB™. The stack model allowed the simulation of the event of a load change to the stack. During the decrease of the current from 400 A to 200 A in 100 s the stack started following the nominal voltage curve, but soon the response transited beyond the nominal value. It was concluded that in some situations the voltage output may be situated outside the safe operating area. Padulles et al.[7] stated the need for a trade-off between the needs of the network and the integrity of the SOFC stack. Dynamic modeling and evaluation of Solid Oxide Fuel Cell combined Heat and Power system operating strategies were also analysed by Nanaeda et al.[3]. A fully integrated dynamic model resolved the physical states, thermal integration and overall efficiency of system to understand the limits and flexibility of the SOFC based CHP system. The simulation results indicated that the grid-support strategy was able to achieve greater than 80% overall system efficiency with the export of electricity to the utility grid. The week averaged total system efficiency was 71.9%[3]. The analysis of the dynamic behaviour of SOFCs, which presents results related to variable power demand, is essential for the positive control of the system. Such modeling under transient conditions was given by D'Andrea et al.[8]. The dynamic model of a poly-generation system based on a biogas fed SOFC plant with CO_2 capture and re-use was analysed in off-design conditions. The impact of a possible malfunction of the coolant air regulation system, the stack performance under different degrees of direct internal reforming and the influence of a sudden current load change were considered to study the plant behaviour. The direct internal reforming of biogas fuel in the SOFC stack was simulated up to 60% of direct methane conversion into the fuel cell anode. It was found that by feeding more biogas directly to the fuel cell, endothermic reforming reactions were promoted which sunk the internal heat generation of the stack thus limiting the risk of stack overheating. In addition, by increasing the direct internal reforming ratio from 0% to 60%, the air flow rate was reduced by 14%. It was proven that a reduced cathode

air flow rate would entail a lower parasitic loss from the air blower and it would also save about 14% of the electric power supplied to the air blower[8]. Recently, the utilization of biogas instead of fossil fuels in a Solid Oxide Fuel Cell based CHP system was tested by Wang et al.[9]. The system model integrated a multi-scale hierarchical 3D SOFC stack model with 0D balance of power component models such as a pre-reformer, a post-burner, an evaporator, a mixer, heat exchangers. The model enables investigation of the overall system performance and stack internal distributed properties down to the electrode scale. The system electrical efficiency and CHP efficiency reached 55.6% and 85%, respectively. It was noticed that the increase of the steam to carbon, S/C, ratio led to a decrease of both system electrical and CHP efficiency and an increase of the stack temperature gradient. Wang et al.[9] stated that the S/C ratio should be set near the minimum S/C ratio to ensure relatively high efficiency and an increased CHP efficiency. They also found that the increase of operation voltage led to the decrease of the system electrical efficiency and the stack temperature gradient, but an increase of the system CHP efficiency[9]. A review of SOFC numerical models can be found in the literature[10–12], while critical aspects of dynamic stability analysis and control of SOFC power plant was described in the literature[13–14].

This study develops a modeling approach to reproduce the dynamic behaviour of a proof-of-concept CHP system based on two-stage SOFC stacks. An integrated system, in which two SOFC stacks are the core elements of a more complex structure with Catalytic Partial Oxidation, CPO_X, reformer and Steam Reformer, SR, units running simultaneously. As discussed in the literature[3, 6] the dynamic system analysis should be readily responsive to electrical load change, thus a novel calculation algorithm was developed in Aspen Dynamics to meet these purposes. The developed approach guarantees high accuracy and quick calculations. To do so, several technical assumptions were used as described in Part 2. Numerical approach. Each component models of SOFC stacks, CPO_x and SR reformers, heat exchangers and burner have been validated making use of the data[18] results obtained from the first of a kind proof-of-concept of this system developed by project partners[15–16, 18]. The validated model has been used to investigate the performance of two-stage SOFC stacks based CHP system in specific conditions. In particular, the following conditions have been analyzed: (i) the stack performance under different load operations of 100% and 47% and under three different values of temperature: 800°C, 830°C and 860°C, (ii) the influence of a fuel utilization factor, FU, change, (iii) the stack performance under different degrees of CPO_x reforming. The present dynamic model allows accurate and fast estimation of stacks performance under various transient operating conditions.

SYSTEM DESIGN

A system layout was developed in an Aspen Dynamics v8.4 Simulation Tool and is provided in Fig. 1. The Combined and Heat Power, CHP, system was constituted by a fuel pre-treatment section (including a Catalytic Partial Oxidation, CPO_x, reformer named "CPOX", a heat exchanger system acts as Steam Reformers, SR, named "SR1" and "SR2" and a burner named "BURNER"), two-stage SOFC stacks containing 90 and 240 fuel cells of 2488 and 4653 W_{el} each, respectively, named "ANODE1" – "CATHODE1" and "ANODE2" – "CATHODE2", several flow split modules to separate natural gas or air: "SP1", "SP2", "SP3", mixers to mix the exhaust gases with natural gas or the cathode gas with the air: "B1", "B3", "M1", "E3" and the heat exchangers for the heat transfer modelling "H-SOFC-1", "H-SOFC-2". The fuel used in the system was natural gas "NG" with a composition of 98.3% CH_4, 0.5% C_2H_6, 0.3% C_3H_8, 0.1% C_4H_{10}, 0.8% N_2; and the air mixture "AIR" was considered as 21% O_2 and 79% N_2. The molar flow rate was equal to 0.018024 mol · s^{-1} at the pressure of 1.04 bar and 0.3922 mol · s^{-1} at the pressure of 1.00 bar, for fresh fuel and air, respectively. The Aspen Dynamics does not have a ready fuel cell model that represents the Solid Oxide Fuel Cell. Therefore, the model proposed by Zhang et al.[17] was used to characterized SOFC by two separate blocks of anode represented by an Equilibrium Reactor model and named "ANODE1" and "ANODE2" as well as a cathode represented by a Separator model and named: "CATHODE1" and "CATHODE2". The mathematical model enables calculations of the current-voltage characteristic of the fuel cell and it was implemented in the "flowsheet constants" compiler window, which supports the Fortran, C and C++. In the model additional calculation code corresponding to the lambda number calculations in the CPO_x reforming sub-system was included. Moreover, to maintain specific steam to carbon, S/C, ratio value, an additional *PIDincr* regulator has been implemented in the supply stream of the steam reforming sub-system, which is connected to the "SP2" splitter.

A compressor called "C1" simulated using *Comp* model has been defined to increase the pressure of the "AIR" stream to 1.04 bar as the "AIR1" stream. There are two *FSplit* distributors called "SP2" and "SP3" to supply enough natural gas and air to the CPO_x reformer with a lambda number, λ_{O_2C}, the value of 0.3092[4]. The lambda number represented the molar ratio of the air to carbon entering the CPO_x reformer and it was defined by equation (1)[15]:

$$\lambda_{O_2C} = \frac{0.21 \cdot \dot{V}_{air}}{(2 \cdot x_{CH4} + 3.5 \cdot x_{C2H6} + 5 \cdot x_{C3H8} + 6.5 \cdot x_{C4H10}) \cdot \dot{V}_{NG}} \quad (1)$$

where: $\dot{V}_{air}$ and $\dot{V}_{NG}$ were the volume flow rates of the air and natural gas entering the CPO_x reformer, at normal conditions 0°C and 1.01325 bar, X_i is the molar fraction of i – components.

The "NG" stream entering to "SP2" splitter and was divided into two streams. The first steam "NG-CPOX" was directed to the CPO_x reforming sub-system. The second pure natural gas stream, "NG-SR", was directed to the blender "E3", where it mixed with the exhaust stream leaving the first SOFC stack.

In the case of Steam Reforming, SR, the value of the S/C coefficient was calculated to meet in SR subsystem the desired oxygen/carbon ratio value using Aspen Dynamics – *PIDincr* functions. Too low S/C ratio inflicts soot formation on the reforming catalyst. The calculated S/C ratio 1.5937, thus desired S/C ratio

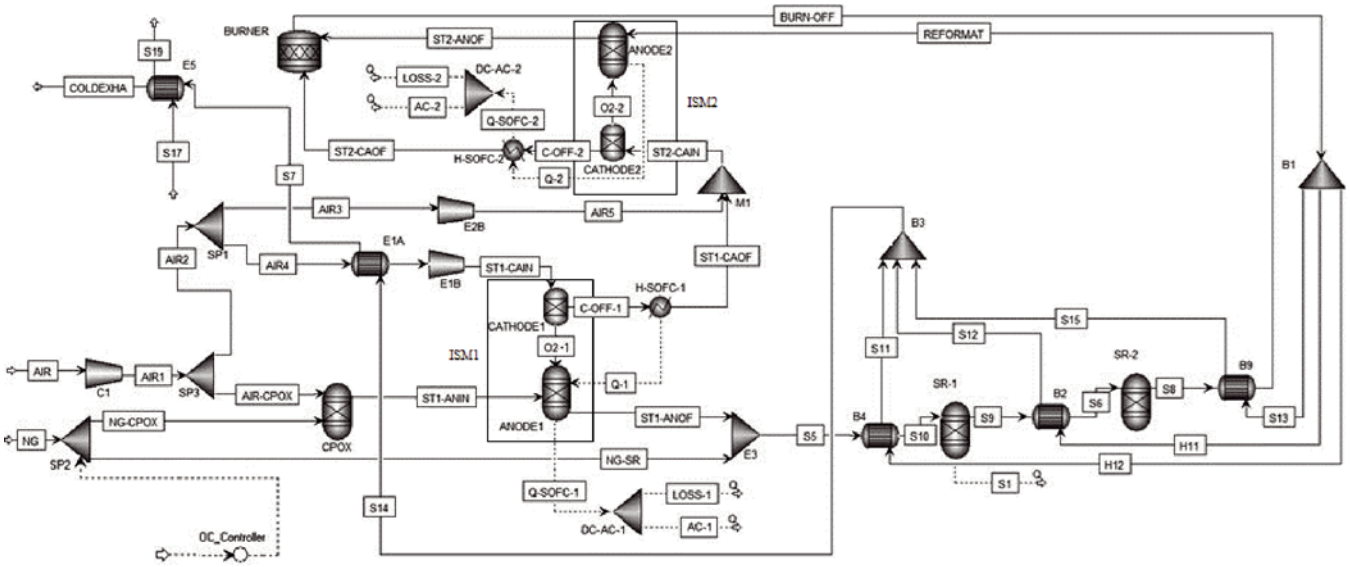

Figure 1. Aspen Dynamics two-stage SOFC stacks based CHP system model flow sheet. Solid lines represent material streams and dotted lines energy streams

value was assumed as 1.60 with an accuracy of 0.01[18] according to equation (2):

$$S/C = \frac{2\cdot n_{CO2}+n_{CO}+n_{H2O}}{n_{CO}+n_{CO2}+1\cdot n_{CH4}+2\cdot n_{C2H6}+3\cdot n_{C3H8}+4\cdot n_{C4H10}} \quad (2)$$

where: n_i – the molar flow of the i-th components in stream "S5".

To distribute the clean air stream "AIR", a "SP3" distributor has been implemented. The exhaust streams from the "SP3" were: "AIR-CPOX" and "AIR2". The first outlet stream was addressed to the CPO_x reforming sub-system. The molar flow rate of "AIR-CPOX" was calculated based on equation (3):

$$\dot{V}_{air} = \frac{(2\cdot x_{CH4}+3.5\cdot x_{C2H6}+5\cdot x_{C3H8}+6.5\cdot x_{C4H10})\cdot \dot{V}_{NG}\cdot \lambda_{O_2C}}{0.21} \quad (3)$$

where: X_i – the molar fractions of the i-th components, was defined as an import variable. The numerical values of the molar fractions of the components were automatically taken by the process simulator from the stream "NG-CPOX".

The second exhaust stream from "SP3", which was the residual "AIR2" stream, was directed to the next divider "SP1" to split into two independent streams: "AIR4" and "AIR3". Those streams were delivered the air respectively to the first and second stacks.

To calculate the desired DC power two *flowsheet constraints* blocks were used in Aspen Dynamics tool. Separated *flowsheets constraints* allowed to estimate the voltage-current parameters for the first SOFC stack containing 90-cells and for the second 240-cells SOFC stack, respectively. The DC-AC power inverter efficiency was assumed to 95% for both stacks. The system operated at fixed stacks temperature of 800, 830 and 860°C and at fixed fuel utilization factor of 75%. The fuel utilization factor, FU, was defined from equation (4) and implemented into the Aspen Dynamics directly in flowsheet constraints:

$$FU = \frac{n_{H_{2,consumed}}}{n_{H_{2,equivalent}}} \quad (4)$$

where: $H_{2,equivalent}$ was the known equivalent H_2 flow rate, thus using the known fuel utilization factor, FU, the amount of H_2 consumed, $H_{2,equivalent}$, in the anode stack was calculated from the equations (5)–(7):

$$n_{H_{2,consumed}} = n_{H_{2,equivalent}} - n_{H_{2,depleted}} \quad (5)$$

$$n_{H_{2,equivalent}} = n_{H_2,anode,inlet} + 1\cdot n_{CO,anode,inlet} + 4\cdot n_{CH_4,anode,inlet} + 7\cdot n_{C_2H_6,anode,inlet} + 10\cdot n_{C_3H_8,anode,inlet} + 13\cdot n_{C_4H_{10},anode,inlet} \quad (6)$$

$$n_{H_{2,depleted}} = n_{H_2,anode,outlet} + 1\cdot n_{CO,anode,outlet} + 4\cdot n_{CH_4,anode,outlet} + 7\cdot n_{C_2H_6,anode,outlet} + 10\cdot n_{C_3H_8,anode,outlet} + 13\cdot n_{C_4H_{10},anode,outlet} \quad (7)$$

BALANCE OF PLANT COMPONENT MODELS

Reformer CPO_x

The CPO_x reformer was modeled by considering Catalytic Partial Oxidation reforming reactions using the equilibrium reactor module *RGibbs* acting at the pressure of 1.04 bar. The following chemical reactions were specified in the CPO_x reformer block:

$$CH_4 + 0.5O_2 \rightarrow 2H_2 + CO \quad (R1)$$
$$CH_4 + 2O_2 \rightarrow 2H_2O + CO_2 \quad (R2)$$
$$2H_2 + O_2 \rightarrow 2H_2O \quad (R3)$$
$$2CO + O_2 \rightarrow 2CO_2 \quad (R4)$$
$$C_2H_6 + O_2 \rightarrow 3H_2 + 2CO \quad (R5)$$
$$C_2H_6 + 3.5O_2 \rightarrow 3H_2O + 2CO_2 \quad (R6)$$
$$C_3H_8 + 1.5O_2 \rightarrow 4H_2 + 3CO \quad (R7)$$
$$C_3H_8 + 5O_2 \rightarrow 4H_2O + 3CO_2 \quad (R8)$$
$$C_4H_{10} + 2O_2 \rightarrow 5H_2 + 4CO \quad (R9)$$
$$C_4H_{10} + 6.5O_2 \rightarrow 5H_2O + 4CO_2 \quad (R10)$$

The value of the lambda number was calculated using equations implemented directly in Aspen Dynamics, in flowsheet constraints. The temperature and composition of the stream leaving "CPOX" (stream "ST1-ANIN") was calculated automatically by Aspen Dynamics. The syngas

produced in the CPO_x reformer and the oxidant "ST1-CAIN" were supplied to the first SOFC stack modelled through the "CATHODE1", "ANODE1" and heater "H-SOFC-1" units, where the electrochemical reaction took place producing the demanded electrical power.

First SOFC stack

The first SOFC stack model named "ISM1" included two separate calculation blocks. The "CATHODE1" block was modelled using available in Aspen Dynamics model of Separator labeled *SEP*. The model assumed the distribution of the input stream "ST1-CAIN" to two independent streams defined as "O2-1" and "C-OFF-1". The "ANODE1" block was characterized by the equilibrium reactor module *RGibbs*, where the electrochemical reactions were specified (R11) – (R15):

$$H_2 + 0.5O_2 \rightarrow H_2O \quad (R11)$$

$$CH_4 + H_2O \rightarrow 3H_2 + CO \quad (R12)$$

$$CO + H_2O \rightarrow H_2 + CO_2 \quad (R13)$$

$$H_2 + CO_2 \rightarrow CO + H_2O \quad (R14)$$

$$H_2O \rightarrow H_2 + 0.5O_2 \quad (R15)$$

The pressure was assumed as 1.03 bar for the first SOFC stack, while the temperature value calculated during the simulation was 834.84°C. The outlet temperature of the exhaust gas "ST1-ANOF" was calculated by using an Aspen Dynamics. The calculations are based on the specified value of the electrical power and the total heat losses. The application of the equations in flowsheet was also required due to the need to specification the amount of the air stream transferred from the cathode to the anode assuming the fuel utilization factor equals to FU = 0.75. In addition, calculation code was used to maintain the operating cathode temperature to the value of the cathode inlet stream temperature "ST1-CAIN" as well as to maintain the outlet temperature values from anode "ST1-ANOF" and cathode "ST1-CAOF". To achieve this assumption, a heater named "H-SOFC-1" was defined for appropriate modelling the heat transfer inside "ISM1". A pressure drop was specified for each side of the SOFC and based on the values obtained from the project partner. For the anode, it was assumed of 0.01 bar, while for the cathode 0.005 bar, respectively. The power produced by the first SOFC stack "ISM1" was calculated by Aspen Dynamics. The power term was represented as the heat stream "Q-SOFC-1". The stream "Q-SOFC-1" in watts W was directed to the DC/AC converter to converts from AC power using the inverter efficiency of 95%. The outlet stream "LOSS-1" represents 5% of the loss of the converter, while the stream "AC-1" represents the electrical AC power in watts.

Steam reforming, SR

The exhaust stream from the cathode of the first SOFC stack, "ST1-ANOF", together with the pure fuel partial flow, "NG-SR" has been directed to a blender called "E3". The resulting "S5" stream was aimed at powering the stream reforming sub-system. A mathematical model for simulating the steam reforming sub-system assumed the contribution of three independent heat exchangers ("B4", "B2", "B9") and two reactors *RGibbs*: "SR-1" and "SR-2". The introduction of an additional reactor into the steam reforming sub-system was intended to increase the degree of hydrocarbon and carbon monoxide overreaction of the system. The steam reforming sub-system consists also of a divider "B1" and a mixer "B3". The divider "B1" was required to distribute the outlet stream from the burner "BURN-OFF" to three independent streams "H11", "H12" and "S13" which were then directed to heat exchangers. While the mixer "B3" was needed in the sub-system to collect the exhaust streams "S11", "S12" and "S15" from the heat exchangers. The use of the cascade solved problems with a high degree of air consumption in the second SOFC stack as well as allowed to reduce the SOFC temperature and risk of catalyst damage. In addition, it also solved the need for heat for endothermic steam reforming reactions (R16) – (R19). In both steam reforming reactors modelled using the *RGibbs* module the following reactions (R16) – (R20) were considered:

$$CH_4 + H_2O \rightarrow 3H_2 + CO \quad (R16)$$

$$C_2H_6 + 2H_2O \rightarrow 5H_2 + 2CO \quad (R17)$$

$$C_3H_8 + 3H_2O \rightarrow 7H_2 + 3CO \quad (R18)$$

$$C_4H_{10} + 4H_2O \rightarrow 9H_2 + 4CO \quad (R19)$$

Water – Gas Shift, WGS:

$$CO + H_2O \rightarrow CO_2 + H_2 \quad (R20)$$

Second SOFC stack

The second SOFC stack named "ISM2" was modelled similar to the first one, which means that the "CATHODE2" was modelled as an oxygen separator using *Separator* block, while the "ANODE2" was modelled as an equilibrium reactor *RGibbs.* The stream coming out from the cathode "ST1-CAOF" block was directed to the Mixer "M1", where it was connected with the fresh air stream "AIR5". A mixed stream "ST2-CAIN" was supplied to the cathode side in the second SOFC stack "ISM2". The SOFC stack included also a third component such as a heater module named "H-SOFC-2" for proper heat exchange modelling. To ensure correct calculation of the second SOFC stack additional computing code was implemented to maintain the appropriate operating conditions. The pressure drop for the anode and cathode were assumed as 0.005 and 0.02 bar, respectively. The following operating value for pressure 1.01 bar was used for simulation. During the calculations, it was assumed equal to the temperature between both SOFC stacks. The electrical power produced by the second SOFC stack was determined by a "Q-SOFC-2" stream. The anode resulting electrochemical flux was then directed to the DC/AC inverter, which was defined as the "DC--AC-2" splitter for simulation purposes. The efficiency of the inverter was assumed as 95%. The streams coming from the splitter, "AC-2" and "LOSS-2" followed by the electrical power of the second stack given for alternating current and 5% of inverter losses.

Burner

Both outlet streams from the second SOFC stack: "ST2-ANOF" and "ST2-CAOF" were delivered to the burner "BURNER". The unit was modelled using the *RStoic* reactor model available in the Aspen Dynamics assuming adiabatic conditions and the heat duty was

equal to 0 W, while the working pressure was assumed equal to 1.01 bar. The burner was used as a combustor and the following reactions have been considered:

$$H_2 + 0.5O_2 \rightarrow H_2O \quad \text{(R21)}$$

$$CO + 0.5O_2 \rightarrow CO_2 \quad \text{(R22)}$$

The outlet stream named „BURN-OFF" had high temperature of 1019.55°C and it was appropriate to direct this steam to the steam reforming sub-system to use the resulting sub-system waste energy. To make full use of waste energy, the CHP system provides an additional apparatus in the form of the divider "B1", which allows the distribution of the stream into three independent streams: "S13", "H11" and "H12" already discussed (Steam reforming, SR).

CALCULATION OF CELL VOLTAGE AND CURRENT

The fuel cell voltage calculation is the core of SOFC based CHP system modeling. The method adopted in the proposed model can be found in the literature[17–19]. It utilizes a performance curve obtained by interpolation of data[18] at standard operating conditions and then predicts the cell voltage by using semi-empirical correlations accounting for the performance adjustments due to the specified operating conditions. This method allows to predict SOFCs performance by implementing semi-empirical equations in Aspen Dynamics, directly in *flowsheet constraints*. The implemented model enables to account for the effect of operating pressure, temperature, current density and fuel/air compositions on the actual voltage. The net voltage, V, was calculated from equation (8):

$$V = V_N - V_{Ohm} - V_{Act} - V_{Conc} \quad (8)$$

where: V_N – Nernst voltage, V_{Ohm} – Ohmic voltage loss, V_{Act} – activation loss, V_{Conc} – concentration loss.

The Nernst voltage, V_N, was determined by the Gibbs free energy change of the H_2 oxidation reaction based on the species mole fraction and the temperature of the SOFC (9):

$$V_N = E_0 + \frac{R \cdot T}{2 \cdot F} \ln\left(\frac{p_{H_2} \cdot p_{O_2}^{0.5}}{p_{H_2O}}\right) \quad (9)$$

where: E_0 – the reversible potential at standard conditions of 1 bar, V, 2 – represents the number of electrons produced per mole of hydrogen fuel reacted, T – the average SOFC temperature, K, R – the molar gas constant, R = 8.314 J · mol^{-1}K^{-1}, p_i – the partial pressure of gases i – component, bar. The reversible potential, E_0, was determined from equation (10)[20]:

$$E_0 = \frac{4184 \cdot [58.3 - (0.0113 + 9.6 \cdot 10^{-7} \cdot T) \cdot T]}{2F} \quad (10)$$

The Ohmic loss, V_{Ohm}, was calculated from equation (11) and were caused by the resistance to electron flow through the anode, cathode and the interconnects and the resistance to ion flow through the electrolyte:

$$V_{Ohm} = \frac{i_{cell}}{A_{cell}}\left(\rho_{anode} \cdot l_{anode} + \rho_{cathode} \cdot l_{cathode} + \rho_{interconn} \cdot l_{interconn} + \rho_{electrolyte} \cdot l_{electrolyte}\right) \quad (11)$$

where: i_{cell} – the cell current, A, A_{cell} – the total active cell surface, m^2, l_i – the i – component thickness, m, ϱ_i – the i – component resistivity calculated as a function of temperature (equations (12) – (15)[21]):

$$\rho_{anode} = 2.98 \cdot 10^{-5} \exp\left(-\frac{1392}{T}\right) \quad (12)$$

$$\rho_{cathode} = 8.114 \cdot 10^{-5} \exp\left(\frac{600}{T}\right) \quad (13)$$

$$\rho_{interconnectors} = 1.2568 \cdot 10^{-3} \exp\left(\frac{4690}{T}\right) \quad (14)$$

$$\rho_{electrolyte} = 2.94 \cdot 10^{-5} \exp\left(\frac{10350}{T}\right) \quad (15)$$

While the cell current was calculated from equation (16):

$$i_{cell} = 4 \cdot F \cdot n_{O_2 required} \quad (16)$$

where: $n_{O_2 required}$ – the oxygen flow rate required calculated from equation (17):

$$n_{O_2 required} = 0.5 \cdot FU \cdot n_{H_2, equivalent} \quad (17)$$

The activation voltage loss, V_{Act}, was mainly associated with the slow of chemical reactions taking place on the surface of the electrodes and was expressed by the equation (18):

$$V_{Act} = \left(\frac{RT}{2\alpha_{anode}F}\right)\ln\left(\frac{j}{j_{0,anode}}\right) - \left(\frac{RT}{4\alpha_{cathode}F}\right)\ln\left(\frac{j}{j_{0,cathode}}\right) \quad (18)$$

where: α – a pre-exponential factor for anode and cathode, j_0 – the exchange current density, A · m^{-2} given by equations (19) – (20):

$$j_{0,anode} = j^*_{H_2} \cdot \left(\frac{p_{H_2}}{p_{ref}}\right) \cdot \left(\frac{p_{H_2O}}{p_{ref}}\right) \cdot \exp\left(-\frac{E_{anode}}{RT}\right) \quad (19)$$

$$j_{0,cathode} = j^*_{O_2} \cdot \left(\frac{p_{O_2}}{p_{ref}}\right)^{0.25} \cdot \exp\left(-\frac{E_{cathode}}{RT}\right) \quad (20)$$

where: p_{ref} – the system reference pressure, p_{ref} = 1 bar, p_i – the i – component partial pressure, $E_{anode/cathode}$ – the anode or cathode energy activation, J · mol^{-1}, j* – the pre-exponential factor, A · m^{-2}.

The concentration loss, V_{Conc}, because of depletion of the reactant concentration at the reaction sites was determined to be (21) – (23):

$$V_{Conc} = V_{Conc\_anode} + V_{Conc\_cathode} \quad (21)$$

$$V_{Conc\_anode} = -\frac{RT}{2F}\ln\left(1 - \frac{j}{j_{limAnode}}\right) + \frac{RT}{2F}\ln\left(1 + \frac{j \cdot p_{H_2}}{j_{limAnode} \cdot p_{H_2O}}\right) \quad (22)$$

$$V_{Conc\_cathode} = -\frac{RT}{4F}\ln\left(1 - \frac{j}{j_{lim\,Cathode}}\right) \quad (23)$$

where: j_{lim} – the current density, which was obtained with maximum fuel consumption during the reaction. The following equations (24) and (25) were used for the anode and cathode current density, respectively:

$$j_{lim\,Anode} = \frac{2 \cdot F \cdot D_{eff,H_2-H_2O}}{R \cdot T \cdot l_{anode}} p_{H_2} \quad (24)$$

$$j_{\lim Cathode} = \frac{4 \cdot F \cdot D_{eff,O_2-N_2}}{R \cdot T \cdot l_{cathode}\left(p - \frac{p_{O_2}}{p}\right)} p_{O_2} \quad (25)$$

where: $D_{eff,i}$ – the overall effective diffusion coefficient for each gas was calculated using equations (26) – (27):

$$D_{eff,H_2-H_2O} = \frac{\varepsilon}{\tau} D_{H_2-H_2O} \quad (26)$$

$$D_{eff,O_2-N_2} = \frac{\varepsilon}{\tau} D_{O_2-N_2} \quad (27)$$

where: D_{ik} – the ordinary binary diffusion coefficient for both anode and cathode (equations (28) – (29)[22]):

$$D_{H_2-H_2O} = \frac{0.00143 \cdot T^{1.75}}{M_{H_2-H_2O}^{0.5} \cdot \left(\vartheta_{H_2}^{1/3} + \vartheta_{H_2O}^{1/3}\right)^2 \cdot p} \quad (28)$$

$$D_{O_2-N_2} = \frac{0.00143 \cdot T^{1.75}}{M_{O_2-N_2}^{0.5} \cdot \left(\vartheta_{O_2}^{1/3} + \vartheta_{N_2}^{1/3}\right)^2 \cdot p} \quad (29)$$

where: ϑ_{ik} – the Fuller diffusion volume taken as 7.07; 12.7, 16.6 and 17.9 $m^2 \cdot s^{-1}$ for H_2, H_2O, O_2 and N_2, respectively[21]. M_i – the molecular weight, $kg \cdot kmol^{-1}$ for the gaseous component, ε – the porosity, τ – the tortuosity of the electrodes.

$$M_{H_2-H_2O} = \frac{2}{\frac{1}{M_{H_2}} + \frac{1}{M_{H_2O}}} \quad (30)$$

$$M_{O_2-N_2} = \frac{2}{\frac{1}{M_{O_2}} + \frac{1}{M_{N_2}}} \quad (31)$$

The cell current density, j, was calculated according to equation (32):

$$j = \frac{i_{cell}}{A \cdot n} \quad (32)$$

where: A – the active fuel cell surface, n – the number of fuel cell in the first 90-cells SOFC stack and the second 240-cells SOFC stack, respectively.

Two-stage SOFC stacks performances were predicted based on the mathematical model implemented in Aspen Dynamics directly in *flowsheet constraints* compiler window. Table 1 gives the input parameters to the model of the two-stage SOFC stacks.

Table 1. Input parameters of the two-stage SOFC stacks mode

Model parameter	Value	Dimension
Active single fuel cell surface	0.01278	[m^2]
Anode thickness	0.00004	[m]
Cathode thickness	0.00004	[m]
Electrolyte thickness	0.00009	[m]
Interconnection thickness	0.005	[m]
Activation energy for anode/cathode	110 000/120 000	[$J \cdot mol^{-1}$]
Electrode porosity	0.35	[-]
Tortuosity	3.8	[-]
Pre-exponential factor anode/cathode	$2.07 \cdot 10^9/5.19 \cdot 10^8$	[$A \cdot m^{-2}$]

SIMULATION RESULTS AND DISCUSSION

Model verification

The component models of two-stage SOFC stacks have been validated by comparing their performances with the data[18]. The analysis was made of the CHP system operating at a constant rate of fuel consumption factor of 0.75. The temperature for both SOFC stacks was identical and calculated during the simulation. The standard pressure inside the fuel cell was 1.03 bar and 1.01 bar, respectively for the first and the second SOFC stacks. The lambda number, λ_{O_2C}, was equal to 0.31, while the S/C ratio was equal to 1.6. The simulation results for a completed model developed in the Aspen Dynamics v8.4 working under the operation load of 100% and 47% were compared to the data[18] and shown in Tables 2 and 3.

The simulation results for the two-stage SOFC based CHP system operating under 100% load were similar to the data[18]. The electrical power of both SOFC stacks estimated by the Aspen Dynamics Simulator Tool was equal to 2488 W and 4653 W, respectively for the first and second stacks (Table 2). The relative error was 2.60% and 3.00%, respectively, which means that the model prediction results for 100% load were close to the level of data[18].

For the SOFC based CHP system operating under the load of 47%, the power determined from the simulation for the first 90-cells stack was equal to 1241 W, while for the second 240-cells SOFC stack this was 2278 W. The differences in values between the data[18] and simulations results were smaller than for the model operating under the load of 100% and were respectively 1.72% for the first SOFC stack and 2.27% for the second SOFC stack as it can be seen in Table 3. Conversely, the temperature difference increased from 0.58% to 2.27%. The first reason for these discrepancies was attributed to the lack of knowledge of the values of material properties characterizing both electrodes[23]. However, this potential cause was ruled out based on a model sensitivity study, which showed that the effect of changing the porosity and tortuosity values was negligible on fuel cell voltage and fuel cell operating temperature. Therefore, it seems that a reasonable cause of the discrepancy is attributed to the semi-empirical equations (12)–(15) used for ohmic overpotential calculations that produced a good agreement between experimental and simulation data in the range of current density up to 0.3 $A \cdot cm^{-2}$. For the higher values of the current density the agreement is worse. Thus, it should be underlined that applied equations (12)–(15) and the constant parameters appearing in the equations have been published in 2006[21], when the fuel cells were operating at much higher temperatures than currently are tested. Furthermore, zero-dimensional approach used to simulated the two-stage SOFC stacks based on the CHP system assumes certain additional simplifications, including, but not limited to, that the temperature of the anode outlet has to be equal to the cathode stream temperature as well as minimalized free Gibbs energy in all the chemical reactions. Nevertheless, it should be considered that the developed model provides the electrical power value of the CHP system with good accuracy.

Table 2. Dynamics simulation results for 100% load compared to data[18], fuel utilization factor, FU = 0.75

Parameter	Dimensions	Aspen Dynamics results	Data[18]	Deviation %
First SOFC stack, 90-fuel cells				
Voltage – single cell	[V]	0.71	0.70	0.83
Voltage - stack	[V]	63.53	62.67	1.36
Current	[A]	39.16	38.70	0.21
Electrical power	[W]	2488	2425	2.60
Second SOFC stack, 240-fuel cells				
Voltage – single cell	[V]	0.74	0.77	3.75
Voltage - stack	[V]	177.87	183.80	3.23
Current	[A]	26.16	26.10	0.23
Electrical power	[W]	4653	4797	3.00
Overall both stacks				
Gross electrical efficiency	[%]	44.00	44.50	1.12
SOFC temperature	[°C]	834.84	830.00	0.58

Table 3. Dynamics simulation results for 47% load compared to data[18], fuel utilization factor, FU = 0.75

Parameter	Dimensions	Aspen Dynamics results	Data[18]	Deviation %
First SOFC stack, 90-fuel cells				
Voltage – single cell	[V]	0.83	0.82	0.76
Voltage – stack	[V]	74.36	73.91	0.61
Current	[A]	16.69	16.50	1.16
Electrical power	[W]	1241	1220	1.72
Second SOFC stack, 240-fuel cells				
Voltage – single cell	[V]	0.86	0.84	2.05
Voltage – stack	[V]	205.73	201.64	2.03
Current	[A]	11.07	11.10	0.24
Electrical power	[W]	2278	2238	1.79
Overall both stacks				
Gross electrical efficiency	[%]	50.46	49.59	1.75
SOFC temperature	[°C]	848.82	830.00	2.27

The assessment of the accuracy of the mathematical model prediction for two-stage SOFC stacks – CHP system was carried out based on the analysis of the influence of temperature change in the operation of SOFCs assuming three test values: 800°C, 830°C and 860°C. To reach the target temperature, the mole flow of the air stream has been modified. Numerical simulations were carried out for the current density in the range of 0–0.5 A · cm^{-2}. The obtained simulation results are shown in Fig. 2 and 3. An increase in current density lowers a single cell voltage and increases the power density. As shown in Fig. 2 and Fig. 3, an increase in the operating temperature of the fuel cell affects both the voltage of a single fuel cell and the power density over the entire current density range, respectively. The voltage of the fuel cell operating at 800°C showed the lowest values in both SOFC stacks. On the other hand, the highest voltage values of the fuel cell in both SOFC stacks were observed at the operating temperature of 860°C (Fig. 2).

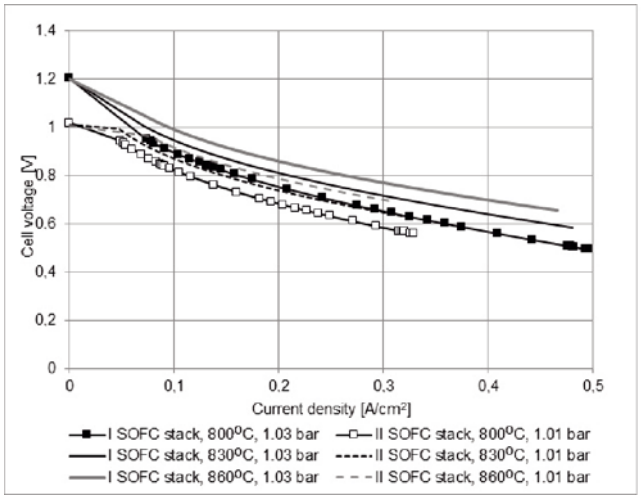

Figure 2. Effect of operation of the first and second SOFC stacks on the single cell voltage at three different operating temperature: 800°C, 830°C and 860°C at fuel utilization factor of 0.75

The same trend was observed for the power density for the tested range of temperature (Fig. 3). In the case of power density, the individual differences were smaller in the range of 0 – 0.2 A · cm^{-2} than in the case of individual voltages for the same current density range. It should be noted that the influence of temperature on the I–V curves is important and has an impact on operating costs in the real system. Due to the operating costs, the operating temperature value of the SOFC should be relatively low around 800°C. This value may extend the life of the stack due to the reduction of thermal stress risk. Moreover, assuming that the temperature value of the fuel stream fed to the first stack was 700.69°C and to the second stack was 700°C, the additional heat was needed to pre-heat the fuel/air stream delivered to the SOFC sub-system to prevent a reduction in an overall CHP system efficiency. As shown in Fig. 3 in the current density range 0.1–0.2 A · cm^{-2}, which is particularly of interest to researchers, the differences in power density were similar for tested temperature values of 800°C, 830°C and 860°C.

The electrical power has been validated for each of the two SOFC stacks for a system operating at 47% and 100% load assuming a constant pressure of 1.03 bar and 1.01 bar for each stack. The temperature values were

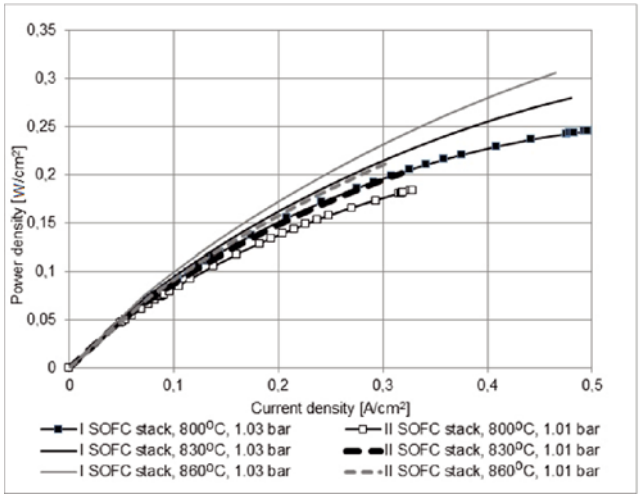

Figure 3. Effect of current density on power density at fuel utilization factor of 0.75 for two-stage SOFC stacks at three different operating temperature: 800°C, 830°C and 860°C

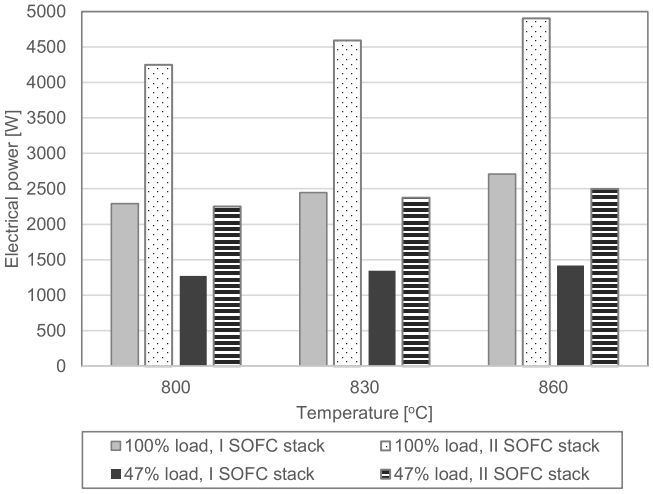

Figure 4. Influence of operating temperature on electrical power generated by both SOFC stacks at fuel utilization of 0.75 and three different operating temperature: 800°C, 830°C and 860°C

800°C, 830°C and 860°C. The results are presented in Fig. 4.

The increase in temperature caused an increase in electrical power of individual SOFC stacks, both at 47% and 100% load (Fig. 4). This does not mean that it is possible to raise the temperature of the SOFC stack to higher values to increase the efficiency of the system without negative consequences involving a significant increase in the risk of overheating and damage to the fuel cells due to thermal stress. As it was mentioned earlier, there have to be a compromise between power, efficiency and system lifetime. Moreover, it can be noticed that when the CHP system was operated under 100% load, there was a significant difference in power generated by the second stack compared to the first SOFC stack (Fig. 4). When both SOFC stacks were operating under 47% load, this difference decreased significantly.

Finally, to gain a high degree of certainty that the defined mathematical model for the two-stage SOFC stacks based CHP systems has been properly implemented in the Aspen Dynamics Process Simulator the gas composition at the inlet to the anode side of the first SOFC stack and steam reformer inlet "S5" stream at 100% load were compared to the data[18]. The results presented in Tables 4 and 5 analysis show good agreement between data[18] and simulated data.

Verification of the compliance of the basic operational parameter prediction has allowed for further advanced research studies including analysis and assessment of the impact of the change in dynamic conditions on the CHP system response.

Effect of the fuel utilization factor on stack and system performance

The first analysis consisted of a prediction of the behaviour of the CHP system operating with a modified fuel utilization factor, FU. The analysis assumed the operation of the CHP system under a constant load, with an initial value of the fuel utilization factor of 0.75 for 10 minutes. Then, over a period of 20 minutes, the value of the fuel utilization factor was gradually increased from 0.75 to 0.85. After stabilization of the final value of the fuel utilization factor, FU, the system was maintained in a steady state for further 5 minutes. After this time, over the next 20 minutes, the value of the fuel utilization factor, FU, was gradually reduced from the set value of 0.85 to the initial value of 0.75. The last 10 minutes of the analysis included maintaining the CHP system in its initial state to obtain the state of so-called stabilization. The following parameters were verified: temperature of fuel outlet stream from first sub-system of SOFC stacks: stream "ST1-ANOF" and "ST2-ANOF", lambda number

Table 4. Comparison of anode inlet ST1-ANIN stream results for 100% and FU of 75% from simulations and data[18]

Parameter	Dimensions	Aspen Dynamics results	Data[18]	Deviation %
Molar flow rate	[mol · s^{-1}]	0.0451	0.0457	1.31
Temperature	[^{0}C]	703.55	710.27	0.95
Pressure	[bar]	1.04	1.04	0.00
Molar composition				
CH_4	[mol · mol^{-1}]	0.0116	0.0109	6.42
C_2H_6	[mol · mol^{-1}]	$8.28 \cdot 10^{-8}$	$5.59 \cdot 10^{-8}$	*
C_3H_8	[mol · mol^{-1}]	$2.05 \cdot 10^{-12}$	$1.19 \cdot 10^{-12}$	*
C_4H_{10}	[mol · mol^{-1}]	$5.03 \cdot 10^{-17}$	$1.67 \cdot 10^{-15}$	*
O_2	[mol · mol^{-1}]	0	0	0.00
N_2	[mol · mol^{-1}]	0.4461	0.4475	0.31
H_2	[mol · mol^{-1}]	0.3290	0.3288	0.06
H_2O	[mol · mol^{-1}]	0.0313	0.0314	0.32
CO	[mol · mol^{-1}]	0.1569	0.1572	0.19
CO_2	[mol · mol^{-1}]	0.0241	0.0242	0.41

*trace

Table 5. Comparison of steam reformer inlet "S5" stream results for 100% load and FU of 75% from simulations and data[18]

Parameter	Dimensions	Aspen Dynamics results	Data[18]	Deviation %
Molar flow rate	[mol · s^{-1}]	0.0556	0.0559	0.54
Temperature	[°C]	657.60	655.22	0.36
Pressure	[bar]	1.03	1.03	0.00
Molar composition				
CH_4	[mol · mol^{-1}]	0.1645	0.1637	0.49
C_2H_6	[mol · mol^{-1}]	$8.37 \cdot 10^{-4}$	$8.30 \cdot 10^{-4}$	*
C_3H_8	[mol · mol^{-1}]	$5.02 \cdot 10^{-4}$	$4.98 \cdot 10^{-4}$	*
C_4H_{10}	[mol · mol^{-1}]	$1.67 \cdot 10^{-4}$	$1.66 \cdot 10^{-4}$	*
O_2	[mol · mol^{-1}]	0	0	0.00
N_2	[mol · mol^{-1}]	0.3625	0.3671	1.25
H_2	[mol · mol^{-1}]	0.0723	0.0716	0.98
H_2O	[mol · mol^{-1}]	0.2413	0.2394	0.79
CO	[mol · mol^{-1}]	0.0372	0.0360	3.33
CO_2	[mol · mol^{-1}]	0.1207	0.1206	0.08

*trace

as well as voltage values of a single cell in both SOFC stacks. The results of the prediction are shown in Fig. 5.

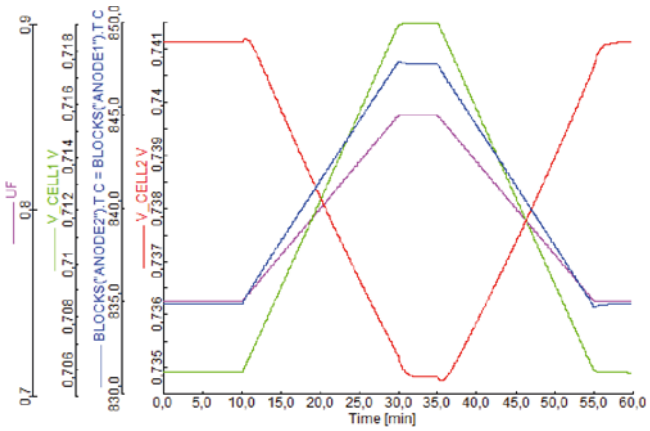

Figure 5. Effect of a fuel utilization factor change in the range of 0.75 to 0.85 on the cell voltage and temperature of the two-stage SOFC stacks based CHP system during the simulation in the transient state in the Aspen Dynamics v8.4 simulator

Assuming a constant value of the feed streams, the temperature of both SOFC stacks increases from 834.84°C to 847.76°C with an increase of the fuel utilization factor. The voltage of a single cell in the first stack gradually increases in contrast to voltage of the second stack. It should be noticed that the change is greater for the first SOFC stack. The reduced amount of hydrogen present in the outlet stream from the first SOFC stack named "ST1-ANOF" results in less hydrogen in the inlet stream to the second SOFC stack, even though steam reforming is included in the CHP system. Consequently, a voltage drop of a single cell in the second stack was observed. However, the significant, 13%, increase the current density in "ISM2" caused the increase of electrical power. For comparison, in "ISM1" it was only 4% as can be seen in Fig. 6.

Increased fuel consumption depletes the fuel stream from the SOFC stacks. Hence, the temperature of the outlet afterburner stream dropped significantly from 1026°C to 963°C. In the presented model the CPO_x reforming process was designed as a sub-system enriching the stream feeding the first SOFC stack, therefore the change of the fuel utilization factor value, in this case, did not affect the value of the lambda number.

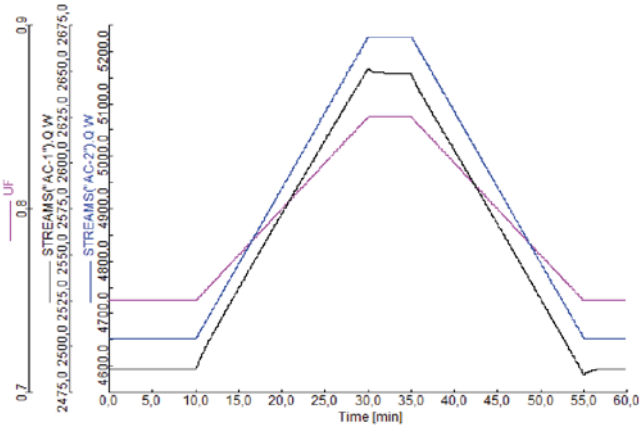

Figure 6. Effect of the fuel utilization factor change in the range of 0.75 to 0.85 on the electrical power in both SOFC stacks, in the transient state in the Aspen Dynamics v8.4 simulator

Effect of lambda number on stack and system performance

The next analysis included changing the value of the lambda number, from an initial value of 0.31 to 0.34. The model of introducing changes was based on the previous analysis: maintain the initial value for 10 minutes, then increasing the value of the lambda number during the next 20 minutes, stabilising the work took place for 5 minutes and gradually restoring the value of the a parameter to the initial value also during 20 minutes. The last 10 minutes were used to stabilise the calculation under the same conditions as assumed during system start-up. Simulation results are shown in Fig. 7.

An increase in the lambda value increased the molar flow rate of the feed stream to the first SOFC stack. This translated into an increase in temperature in both SOFC stacks from 834.84°C to 843.03°C. An increase in the lambda value affects to the higher value of the molar flow rate of the inlet stream of the first SOFC stack. This was due to the higher rate of CH_4 reaction in the CPO_x reactor. As a consequence, although the temperature of the outlet stream from the CPO_x reactor supplying the first SOFC sub-system was approximately 58°C higher, a higher amount of H_2O was generated. Hence, it was required to supply more air to the "ISM1", which had to be heated to the operating temperature of the first SOFC stack. With regard to the first stack,

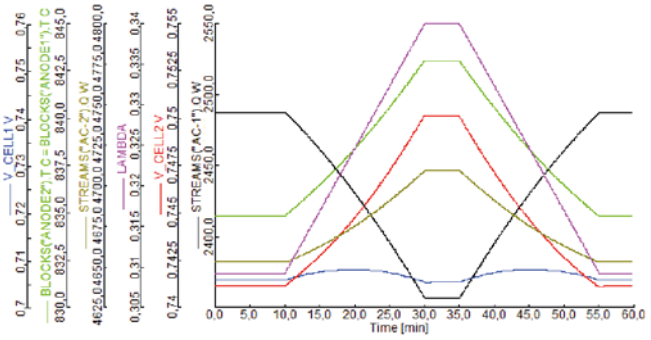

Figure 7. Results of simulation in the dynamic state for the CHP system with a change in the value of the lambda number, λ_{O_2C}, in the range of 0.31–0.34

changes in the voltage were negligible, caused by adjusting the fuel distribution in the "SP2" splitter, the S/C parameter with an accuracy of 0.01. Therefore, electric power of "ISM1" has decreased by 5.27%. Differently, the voltage of a single cell in the second stack has increased. This was due to an increase in the temperature of the air inlet stream fed to the second SOFC stack, "ST2-CAIN". The electric power of "ISM2" has changed from 4653 W to 4709 W, by 1.12%.

CONCLUSIONS

A complete dynamic model of the Combined and Heat Power System based on two-stage Solid Oxide Fuel Cell stacks for the estimation of the plant components characteristics and performance was developed. The SOFC operation involved various complicate multiphysical phenomena including gas diffusions, electrochemical reactions and heat generations. To know and understand the operation characteristics as well as to predict SOFCs performance, an accurate mathematical model was required to be developed. The aim of the work concerning the characterization of the dynamic behaviour in terms of the electrical power was achieved through the model implemented in the Aspen Dynamics Simulator Tool. Particular attention was given to the two-stage SOFC stacks operating conditions in consideration of their transient response.

The Aspen Dynamics model was developed basing on existing Aspen Dynamics unit operation blocks and user defined functions (*i.e. PIDincr)* that allowed to evaluate the thermo-chemical operating conditions of the system at nominal load 100% and 47%. All the system components were implemented in the Aspen Dynamics Simulator Tools to analyse the behaviour of the CHP system at chosen loads. Preliminary simulations were carried out to achieve a right plant components and to evaluate the system global performances consistent with the data[18]. After this phase, the transient performances have been investigated through simulations under an imposed electric load step. The tests carried out considering fuel utilization factor and lambda number variations proved that typical plant operations can be simulated and good agreement with the data[18] was obtained.

This work demonstrates that the developed model can properly predict the performance for the two-stage SOFC stacks based CHP system under different operating conditions. It has been shown that the developed dynamic system model is useful tool to study the limits and flexibility of the CHP system.

NOMENCLATURE

A_{cell} – total active fuel cell surface, [m^2]
$D_{i,k}$ – ordinary binary diffusion coefficient, [m^2s^{-1}]
$D_{eff,i}$ – overall effective diffusion coefficient for i – component, [m^2s^{-1}]
$E_{anode/cathode}$ – anode or cathode energy activation, [V]
F – Faraday's constant, [$C \cdot mol^{-1}$]
i_{cell} – cell current, [A]
i – species H_2, H_2O, O_2, [-]
j – density current, [$A \cdot m^{-2}$]
j_0 – exchange density current, [$A \cdot m^{-2}$]
j* – pre-exponential factor, [$A \cdot m^{-2}$]
j_{lim} – current density at maximum fuel consumption, [$A \cdot m^{-2}$]
l_{anode} – anode thickness, [m]
$l_{cathode}$ – cathode thickness, [m]
$l_{electrolyte}$ – electrolyte thickness, [m]
$l_{interconn}$ – interconnectors thickness, [m]
M_i – molar mass of species *i*, [$kg \cdot mol^{-1}$]
$n_{CH_4,in}$ – molar flow rate of H_2 that could be produced from the CH_4, [$mol \cdot s^{-1}$]
$n_{CO_{in}}$ – molar flow rate of H_2 that could be produced from the CO, [$mol \cdot s^{-1}$]
$n_{H_2,consumed}$ – molar flow rate of H_2 consumed, [$mol \cdot s^{-1}$]
$n_{H_2,equivalent}$ – equivalent H_2 molar flow rate, [$mol \cdot s^{-1}$]
$n_{H_2,in}$ – molar flow rate of H_2, [$mol \cdot s^{-1}$]
$n_{H_2,required}$ – required O_2 molar flow rate, [$mol \cdot s^{-1}$]
p – pressure, [bar]
p_i – partial pressure of gaseous i – component, [bar]
p_{ref} – system reference pressure, [bar]
R – universal gas constant, [$Jkmol^{-1}K^{-1}$]
T – temperature, [K]
U_f – fuel utilization factor, [-]
V – voltage, [V]
V_{Act} – activation loss, [V]
V_{Conc} – concentration loss, [V]
V_N – Nernst voltage, [V]
V_{Ohm} – Ohmic voltage loss, [V]
X_i – molar fraction of i – component, [$mole_i \cdot mole^{-1}$]

Greek symbols

a – conversion energy coefficient into electrical one, [-]
λ_{O_2C} – lambda number, [-]
ρ – resistivity, [$\Omega \cdot m$]
τ – tortuosity factor, [-]
ϑ_{ik} – Fuller diffusion volume, [$m^2 \cdot s^{-1}$]

ACKNOWLEDGMENTS

The research program leading to these results received funding from the European Union's Seventh Framework Programme (FP7/2007-2013) for the Fuel Cells and Hydrogen Joint Undertaking (FCH JU) under grant agreement n° [621213]. Information contained in the paper reflects the only view of the authors. The FCH JU and the Union are not liable for any use that may be made of the information contained therein. The work was also financed from the Polish research funds awarded for project No. 3126/7.PR/2014/2 of international cooperation within STAGE-SOFC in years 2014–2017.

LITERATURE CITED

1. Tu, B., Wen, H., Yin, Y., Zhang, F., Su, X., Cui, D. & Cheng, M. (2020). Thermodynamic analysis and experimental study of electrode reactions and open circuit voltage for methane-fuelled SOFC. *Internat. J. Hydrog. Energy*, 45, 58, 34069–34079. DOI: 10.1016/j.ijhydene.2020.09.088.

2. Lee, K., Kang, S. & Ahn, K.Y. (2017). Development of a highly efficient solid oxide fuel cell system. *Appl. Energy*, 205, 822–833. DOI: 10.1016/j.apenergy.2017.08.070.

3. Nanaeda, K., Mueller, F., Brouwer, J. & Samuelsen, S. (2010). Dynamic modeling and evaluation of solid oxide fuel cell – combined heat and power system operating strategies. *J. Power Sourc.*, 195, 3176–3185. DOI: 10.1016/j.jpowsour.2009.11.137.

4. Ferrari, M.L. (2015). Advanced control approach for hybrid systems based on solid oxide fuel cells. *Appl. Energy*, 145, 364–373. DOI: 10.1016/j.apenergy.2015.02.059.

5. Magistri, L., Traverso, A.F. & Shah, R.K. (2005). Heat Exchangers for Fuel Cell and Hybrid System Applications. *J. Fuel Cell Sci. Technol.*, 3(2), 111–118. DOI: 10.1115/1.2173665.

6. Santis-Alvarez, A.J., Nabavi, M., Hild, N., Poulikakos, D. & Stark, W.J. (2011). A fast hybrid start-up process for thermally self-sustained catalytic n-butane reforming in micro-SOFC power plants. *Energy & Environ. Sci.*, 4, 3041–3050. DOI: 10.1039/C1EE01330K.

7. Padulles, J., Ault, G.W. & McDonald, J.R. (2000). An integrated SOFC plant dynamic model for power systems simulation. *J. Power Sourc.*, 86, 495–500. DOI: S0378-7753(99)00430-9.

8. D'Andrea, G., Gandiglio, M., Lanzini, A. & Santarelli, M. (2017). Dynamic model with experimental validation of a biogas-fed SOFC plant. *Energy Convers. Manag.*, 135, 21–34. DOI: 10.1016/j.enconman.2016.12.063.

9. Wang, Y., Wehrle, L., Banerjee, A., Shi, Y. & Deutschmann, O. (2021). Analysis of a biogas-fed SOFC CHP system based on multi-scale hierarchical modeling. *Renewable Energy*, 163, 78–87. DOI: 10.1016/j.renene.2020.08.091.

10. Kakac, S., Pramuanjaroenkij, A. & Zhou, X.Y. (2007). A review of numerical modeling of solid oxide fuel cells. *Internat. J. Hydrog. Energy*, 32, 761–786. DOI: 10.1016/j.ijhydene.2006.11.028.

11. Ghorbani B. & Vijayaraghavan K. (2019). A review study on software-based modeling of hydrogen-fueled solid oxide fuel cells. *Internat. J. Hydrogen Energy*, 44, 13700–13727. DOI: 10.1016/j.ijhydene.2019.03.217.

12. Grew, K.N. & Chiu W.K.S. (2012). A review of modeling and simulation techniques across the length scales for the solid oxide fuel cells. *J. Power Sourc.*, 199, 1–13. DOI: 10.1016/j.jpowsour.2011.10.010.

13. Safari, A., Shahsavari, H. & Salehi, J. (2018). A mathematical model of SOFC power plant for dynamic simulation of multi-machine power systems. *Energy*, 149, 397–413. DOI: 10.1016/j.energy.2018.02.068.

14. Mehr, A.S., MosayebNezhad, M., Lanzini, A., Yari, M., Mahmoudi, S.M.S. & Santarelli, M. (2018). Thermodynamic assessment of a novel SOFC based CCHP system in a wastewater treatment plant. *Energy,* 150, 299–309. DOI: 10.1016/j.energy.2018.02.102.

15. Posdziech, O. System concepts and BoP components, Staxera/sunfire GmBH, http://slideplayer.com/slide/8883912/

16. Bachman, J., Posdziech, O., Pianko-Oprych, P., Kaisalo, N. & Pennanen, J. (2017). Development and testing of innovative SOFC system prototype with staged stack connection for efficient stationary power and heat generation. *ECS Transactions*, 78, 1, 133–144. DOI: 10.11490/07801.0133ecst.

17. Zhang, W., Croiset, E., Douglas, P.L., Fowler, M.W. & Entchev, E. (2005). Simulation of a tubular solid oxide fuel cell stack using Aspen Plus^{TM} unit operation models. *Energy Convers, Manag.,* 46, (2), 181–196. DOI:10.1016/j.enconman.2004.03.002.

18. STAGE-SOFC: Innovative SOFC system layout for stationary power and CHP applications, EU Project, internal report. 1.04.2014.

19. Huangfu, Y., Gao, F., Abbas-Turki, A., Bouquain, D. & Miraoui, A. (2013). Transient dynamic and modeling parameter sensitivity analysis of 1D solid oxide fuel cell model, *Energy Convers. Manag.*, 71, 172–185. DOI: 10.1016/j.enconman.2013.03.029.

20. Yang, F., Zhu, X.J. & Cao, G.Y. (2007). Nonlinear fuzzy modeling of a MCFC stack by identification method. *J. Power Sourc.*, 166, 354–361. DOI: 10.1016/j.jpowsour.2007.01.062.

21. Cali, M., Santarelli, M.G.L. & Leone, P. (2006). Computer experimental analysis of the CHP performance of a 100 kW_e SOFC field unit by a factorial design. *J. Power Sourc.,* 156, 400–413. DOI: 10.1016/j.jpowsour.2005.06.033.

22. Todd, B. & Young, J.B. (2002). Thermodynamic and transport properties for solid oxide fuel cell modelling. *J. Power Sourc*., 110, 186–200. DOI: 10.1016/S0378-7753(02)00277-X.

23. Janardhanan, V.M. & Deutschmann, O. (2006). CFD analysis of a solid oxide fuel cell with internal reforming: Coupled interactions of transport, heterogeneous catalysis and electrochemical processes. *J. Power*, *Sourc*., 162, 1192–1202. DOI: 10.1016/j.jpowsour.2006.08.017.